Rare Metal Materials and Engineering
Volume 51, Issue 2, February 2022
Available online at www.rmme.ac.cn

Science Press

Cite this article as: Mei Jinna, Xue Fei, Wu Tiandong, et al. A Simple Constitutive Model for FeCrNiMn Medium Entropy Alloy Considering Work-Hardening and Dynamic Softening[J]. Rare Metal Materials and Engineering, 2022, 51(02): 429-435.

ARTICLE

A Simple Constitutive Model for FeCrNiMn Medium Entropy Alloy Considering Work-Hardening and Dynamic Softening

Mei Jinna[1], Xue Fei[1], Wu Tiandong[2], Wei Na[2], Cai Zhen[1], Xue Xiangyi[2]

[1] Suzhou Nuclear Power Research Institute, Suzhou 215004, China; [2] Xi'an Super Crystal Sci-Tech Development Co., Ltd, Xi'an 710200, China

Abstract: The flow behavior of a medium entropy alloy with a nominal composition of $Fe_{0.25}Cr_{0.25}Ni_{0.25}Mn_{0.25}$ was analyzed by isothermal compression performed in the temperature range of 900~1050 °C and strain rate range of 1~0.001 s^{-1}. The results show that the hot deformation is predominated by dynamic recrystallization, so that the flow curves exhibit a single-peak shape as those of other alloys with low stacking-fault energy. Particular emphasis was paid to develop a simple constitutive model which can describe the entire deformation history. For this purpose, the work-hardening behavior as well as the dynamic softening regime were analyzed. With the aid of Kocks-Mecking plots, it is found that the hardening rate of the present alloy is linearly decreased with stress in the work-hardening stage, and hence the stress-strain behavior can be described by the conventional dislocation density-based model. Meanwhile, the softening regime, which is caused by dynamic recrystallization, can be modelled by the classic JMAK equation. Besides, the model is further modified to reduce the number of parameters and simplify the regression analysis. The proposed semi-physical based model can not only accurately predict the stress-strain behavior to strain levels outside the experimental strain range, but can also be promoted to other alloys with low stacking-fault energy.

Key words: medium entropy alloy; hot deformation; flow behavior; constitutive model

In recent fifteen years, there has been considerable interest in multi-principal element alloys (MPEAs) which motivates an alloy-design definition based on the magnitude of entropy[1-3]. The MPEAs have attracted intensive attention due to their unique microstructure and properties[2,3]. Moreover, MPEAs are considered a promising candidate for structural applications, and hence many efforts have been made to tap the up-limit of mechanical performance[4-6]. However, owing to their multi-component, equimolar nature, the MPEAs possess relatively poor castability so that the as-cast microstructure is generally characterized by composition segregation, coarse dendrites, and casting porosity[7-9]. Apparently, these defects are detrimental to their utilization so the thermomechanical treatment is of great significance for microstructural improvements. As a prerequisite for that, a comprehensive understanding of high temperature deformation behavior is required.

In the past decade, in order to determine the hot-working window and processing map, as well as the effects of deformation parameters (strain, strain rate, temperature, etc.) on the microstructure, some works have been performed to investigate the deformation behavior of the MPEAs by means of isothermal compression[10-14]. It is well-established that the flow behavior of MPEAs is a complex process involving work-hardening and dynamic softening. The deformation parameters as well as the initial microstructure can significantly affect the mechanical response of the alloys. Then a constitutive model which permits accurate evaluation of the instantaneous response is needed to reveal the deformation kinetics feature, especially the numerical simulation of the hot-forming processes. Till date, most of the constitutive analyses for MPEAs are performed based on the well-known hyperbolic-sine law[13,14]:

$$Z = \dot{\varepsilon}\exp\left(\frac{Q}{RT}\right) = A\left[\sinh(\alpha\sigma)\right]^n \quad (1)$$

where Z is the Zenner-Hollomon parameter (Z parameter); $\dot{\varepsilon}$ and σ are the strain rate and stress, respectively; R is the universal gas constant and T is the absolute temperature; Q is the apparent deformation activation energy; A, α and n are material constants. Although this equation has been widely

Received date: February 09, 2021
Corresponding author: Xue Fei, Ph. D., Professor, Suzhou Nuclear Power Research Institute, Suzhou 215004, P. R. China, E-mail: xuefei@cgnpc.com.cn

applied to quantify the deformation kinetics, the strain accumulation effect is ignored. That is, the deformation history involving work-hardening and dynamic softening cannot be reflected by Eq. (1). To address this point, the hyperbolic-sine law has been modified which can be summarized as the following form[15,16]:

$$\dot{\varepsilon}\exp\left[\frac{Q(\varepsilon)}{RT}\right]=A(\varepsilon)\left\{\sinh\left[\alpha(\varepsilon)\,\sigma\right]\right\}^{n(\varepsilon)} \quad (2)$$

where Q, A, α and n are considered to be equations about strain (ε), and generally in the form of quintic polynomial. To obtain the mathematic expression of the abovementioned parameters, multi-linear and nonlinear regression analyses are required for different strain levels within the experimental strain range from which the constitutive expression is derived. The constitutive relationship can be accurately described within the strain range using Eq. (2). However, numerous constants are involved and the regression process is quite complicated. Furthermore, the application of polynomial for material parameters has no physical foundation so that the model based on Eq.(2) is only valid in the experimental strain range. Unreasonable or even illegal constitutive behavior may occur at larger strains [15]. More efforts are required to obtain simpler physical-based constitutive models which can extrapolate the flow curves to high strain level.

For this purpose, the high temperature deformation behavior of a MPEA with medium entropy, $Fe_{0.25}Cr_{0.25}Ni_{0.25}Mn_{0.25}$ [17], was investigated in this work. The work-hardening and dynamic softening stages were analyzed. A constitutive model was developed based on the flow characteristics. The proposed model not only can accurately predict the constitutive behavior, but also is valid beyond the experimental strain range.

1 Experiment

The applied medium entropy alloy is composed of Fe, Cr, Ni and Mn in equal atomic ratios. A ingot with a dimension of Φ90 mm×400 mm was prepared by induction suspension melting (ISM) for two times. After that, the ingot was annealed at 1200 °C for 1 h to mitigate the chemical segregations followed by air-cooling to room temperature. For isothermal compression, samples with a size of Φ8 mm×12 mm were machined from the ingot. The hot compression was performed on a Thermecmastor-Z simulator at temperatures of 900, 950, 1000, 1050 °C. The samples were heated up to target temperatures with a rate of 10 °C/s and held for 5 min to homogenize the temperature. Then the samples were compressed at constant strain rates of 0.001, 0.01, 1 s^{-1} up to a true strain of 1. Lubricants were applied between the sample and the anvils to minimize the friction. During deformation, the true stress-strain curves were recorded in real time. After compression, the samples were sectioned and mechanically polished followed by electrolytic polishing for microstructure characterization. The microstructure was analyzed on a Zeiss-sigma500 scanning electron microscope (SEM) equipped with electron back-scattered diffraction (EBSD).

2 Results and Discussion

2.1 Microstructure before and after compression

The microstructure of the FeCrNiMn medium entropy alloy before (Fig.1a) and after (Fig.1b~1e) deformation is shown in Fig.1. One can note that the initial microstructure is characterized by a dual-phase morphology with fcc phase as the matrix and bcc phase as the precipitates, and the mean size of them is ~100 and ~20 μm, respectively. After deformation at high strain rates and low temperatures, both the fcc and bcc phases are significantly elongated accompanied by the occurrence of dynamic recrystallization (DRX), forming a typical necklace structure surrounding the deformed grains. Meanwhile, a fully DRX structure is obtained when deformed at low strain rates and high temperatures. Besides, with increasing the temperature and decreasing the strain rate, the DRX grain size noticeably increases. Based on these metallographic observations, one may conclude that the hot deformation of the present medium entropy alloy is predominated by DRX.

2.2 Flow behavior

The obtained true stress-strain curves are shown in Fig. 2. One can note that in the experimental range, the stress is quite sensitive to the deformation parameters. As the strain rate increases and temperature decreases, the stress is evidently increased. As a class of alloys with low stacking fault energy[14], it is not surprising that the flow curve of the present alloy is characterized by a single stress-peak. That is, the flow stress is increased abruptly in the initial deformation stage up to a peak value, and then the alloy is continuously softened before reaching the steady-state plateau. It is consistent with the metallographic observations that DRX is predominant during deformation.

The appearance of stress peak on the flow curve due to DRX is schematically illustrated in Fig.3. At the beginning of straining, the crystal defects are rapidly accumulated accompanied by insufficient but increased dynamic recovery (DRV). As a result, a work-hardening stage appears, though the corresponding hardening rate (θ) is continuously decreased. Assuming that the deformation is solely controlled by dynamic recovery (DRV), the plastic flow path should go along the red curve (σ^{DRV}) in the figure, until reaching a steady-state flow with a stress level corresponding the so-called saturation stress (σ^*)[18]. However, the situation is changed due to DRX. The onset of DRX is a consequence of the critical defect density arising from work-hardening, and the corresponding critical strain (ε_c) is roughly 0.8 times larger than the peak strain (ε_p)[18]. With the proceeding of DRX, the work-hardening rate decreases down to negative, leading to the presence of stress peak (σ_p) as well as the flow softening. However, the hardening rate is gradually increased at a certain infection point (ε_I) and when 100% DRX is attained, the hardening rate approaches zero and the stress-strain curve exhibits a persistent steady-state flow (σ_s) after that.

2.3 Work-hardening

As mentioned above, the work-hardening stage can be

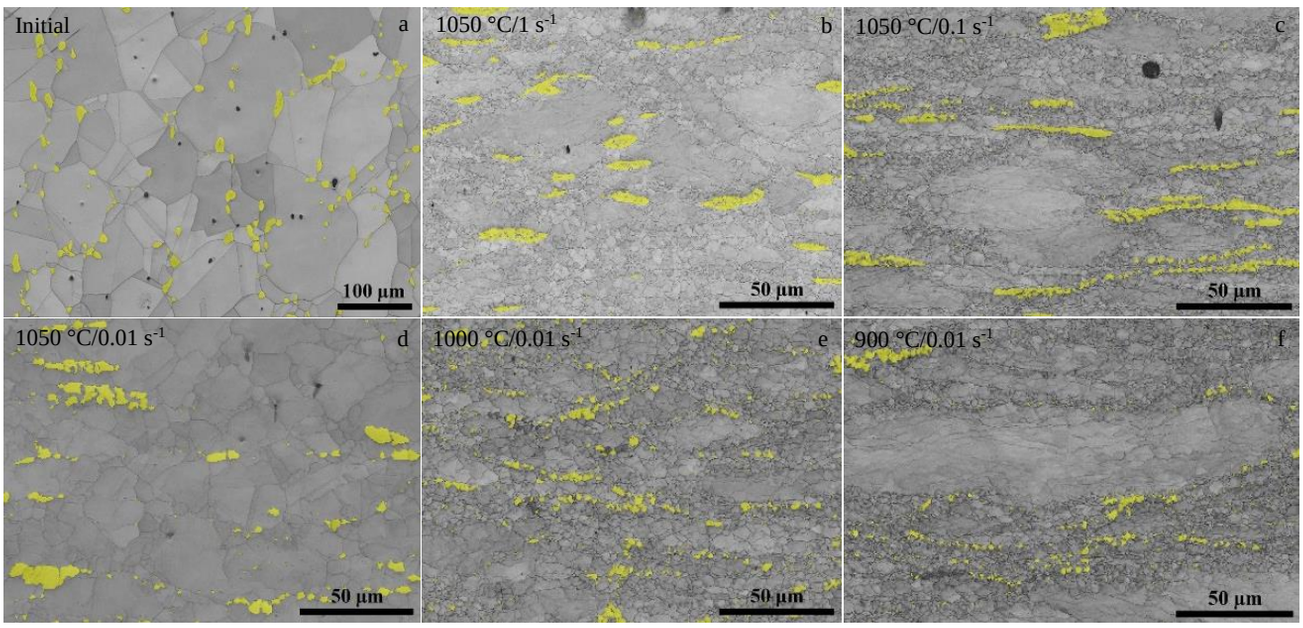

Fig.1 Band contrast maps of the alloy before (a) and after (b-f) deformation in various conditions (bcc phase which is yellow colored is superimposed on the maps)

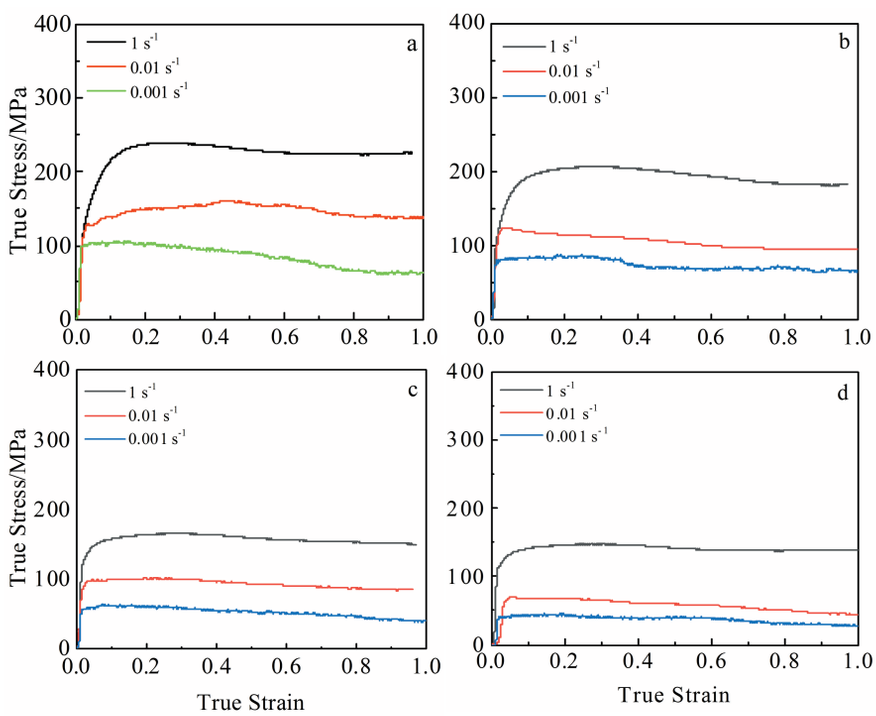

Fig.2 Flow curves of FeCrNiMn medium entropy alloy under various conditions: (a) 900 °C, (b) 950 °C, (c) 1000 °C, and (d) 1050 °C

defined as the flow curve before the stress peak. Its feature is determined by the competitive effect between the accumulation of crystal defects and DRV/DRX, and can be clearly revealed by the Kocks-Mecking plot, i.e., the θ-σ plot. As summarized by Bambach et al[19], there are five typical work-hardening curves according to the morphology of the Kocks-Mecking plot: (i) the hardening rate is linearly decreased with stress; (ii) θ-σ curve shows a concave-up and then concave-down tendency; (iii) concave-up appearance; (iv) concave-down appearance; (v) complex shape. For each case, there is a dislocation density-based model to quantify the stress-strain relationship.

As for the FeCrNiMn medium entropy alloy, the Kocks-Mecking plot corresponding to the work-hardening stage is

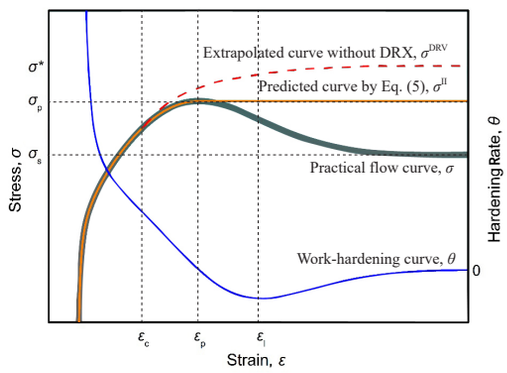

Fig.3 Schematic description of the flow behavior of FeCrNiMn medium entropy alloy

shown in Fig. 4a. One can note that apparently, the work-hardening rate decreases linearly with the stress. This means that the evolution of the dislocation density can be roughly described by the following equation[19]:

$$\rho\frac{\mathrm{d}\rho}{\mathrm{d}\varepsilon} = k_1\sqrt{\rho} - k_2\rho \tag{3}$$

where ρ is the dislocation density, k_1 and k_2 are material constant. The integration of Eq.(3) gives the following form if considering that the applied stress can be related directly to the square root of the dislocation density:

$$\sigma = \sigma_0 + (\sigma^* - \sigma_0)[1 - \exp(-\Omega\varepsilon)] \tag{4}$$

where σ_0 is the initial yield stress, Ω is the DRV coefficient. In the simplest case, one may assume that the material exhibits pure viscosplastic flow because the elastic regime cannot be identified on the present flow curves. Meanwhile, the calculation of saturation stress requires extrapolation and hence cannot be obtained directly from the curves. Therefore, the saturation stress is assumed to be replaced by the peak stress instead. Then the σ^{DRV} curve in Fig.3 will be replaced by the yellow one (σ_H), and Eq.(4) can be simplified to be:

$$\sigma^H = \sigma_p[1 - \exp(-\Omega\varepsilon)] \tag{5}$$

In this equation, the peak stress can be simply modelled by the hyperbolic-sine law. Fig. 5 shows the dependence of the peak stress on the Z parameter. It can be noted that the hyperbolic-sine law gives a good fit to the data. Meanwhile, for each deformation condition, the value of Ω can be directly obtained by linear regression (Fig.4a). Apparently, the Ω value is closely related to the deformation conditions, and can be expressed as a function of the Z parameter, as manifested in Fig.4b.

2.4 Dynamic softening

According to the analysis in Section 2.1 and 2.2, it can be noted that the apparent softening of the flow curves is caused by DRX, and hence the DRX kinetics can be approximately derived from the flow curve by the following method[18]:

$$X = \frac{\sigma^{DRV} - \sigma}{\sigma^* - \sigma_s} \tag{6}$$

where X denotes the DRX volume fraction. Meanwhile, the DRX kinetics can be modelled by the well-known JMAK

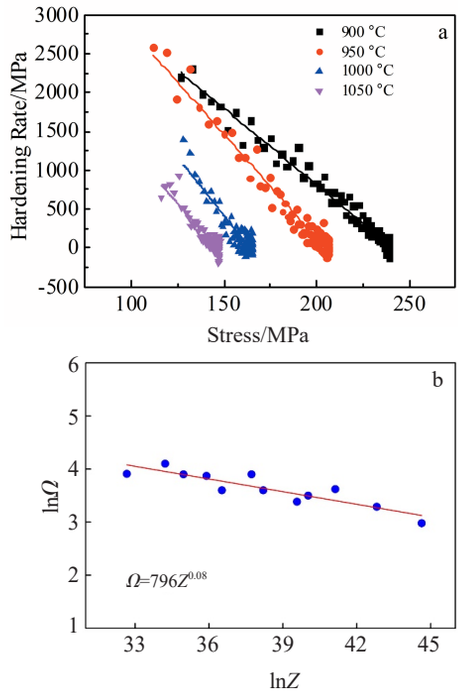

Fig.4 Correlation between hardening rate and stress at various temperatures and strain rate of 1 s^{-1} (a) and dependence of parameter Ω on Z parameter (b)

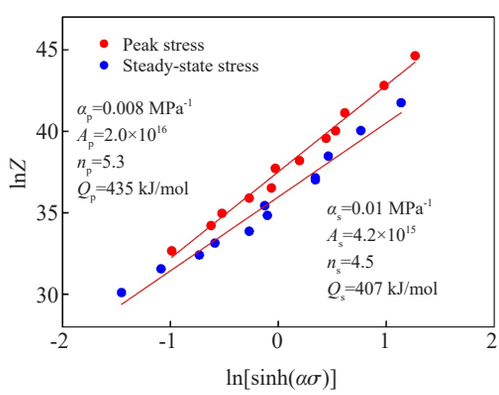

Fig.5 Effect of temperature and strain rate on the peak stress and steady-state stress

equation:

$$X = 1 - \exp\left[-k\left(\frac{\varepsilon - \varepsilon_c}{\varepsilon_p}\right)^n\right] \tag{7}$$

Apparently, the mathematical expression for the flow stress in the softening stage can be derived by combining Eq. (6) with Eq.(7). However, one may notice that some parameters in the equations, such as σ^{DRV} and ε_c, require extrapolation analysis and cannot be readily obtained. Therefore, some simplification treatments are carried out in the present study.

In section 2.2 we have applied the peak stress (σ_p) instead of the saturation stress (σ^*), and hence the derived σ^{DRV} curve

from Eq. (5) should be the same as the σ^{H} curve in Fig.3. This implies that the σ^{DRV} is constantly equal to the peak stress after stress peak. The critical strain ε_c, which is essentially corresponding to the separation point between σ^{DRV} and the practical flow curve, is coincident to the peak strain (ε_p) instead. According to the above simplification, Eq.(6) and Eq. (7) can be replaced by:

$$X = \frac{\sigma^{H} - \sigma}{\sigma_p - \sigma_s} \tag{8}$$

and

$$X_s = 1 - \exp\left[- k\left(\frac{\varepsilon - \varepsilon_p}{\varepsilon_p} \right)^n \right] \tag{9}$$

respectively. Note that the parameter X_s denotes the apparent softening fraction rather than the DRX kinetics.

Analogous to the peak stress, the σ_s in Eq.(8) can also be modelled by the hyperbolic-sine law, as shown in Fig. 5. For the peak strain in Eq. (9), the flow curves shown in Fig. 2 demonstrate that the peak strain is sensitive to the deformation condition. A plot of the peak strain as a function of the Z parameter is shown in Fig. 6 together with the results of regression analysis. A roughly linear relationship can be identified between ln$Z$ and lnε_p.

The parameter k and n in Eq.(9) can be determined by linear regression analysis between ln{ln[1/(1−X_s)]} and ln[(ε−ε_p)/ε_p],

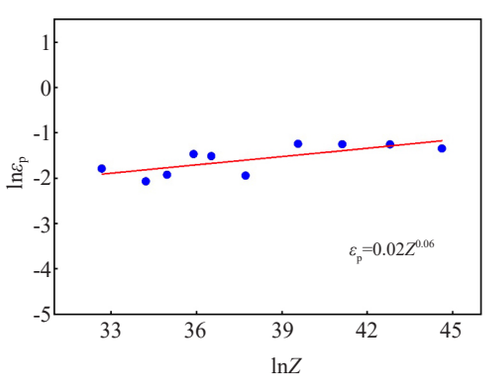

Fig.6 Correlations between the peak strain ε_p and Z parameter

where X_s can be derived from the flow curves using Eq.(8). As shown in Fig. 7a, the values of n are found to be independent of deformation temperature and strain rates, which fall between 1.7 and 2.2 with a mean value of about 2. Meanwhile, the k values are found to be more dispersed but show a weak tendency to decrease with increasing the temperature and decreasing the strain rate, as manifested by the regression analysis shown in Fig.7b.

2.5 Constitutive modelling

According to the above analysis, we have modelled the work-hardening stage and the dynamic softening regime of the present medium entropy alloy. The complete constitutive equation is as follows:

$$\begin{cases} \sigma^{H} = \sigma_p[1 - \exp(-\Omega\varepsilon)] & \varepsilon < \varepsilon_p \\ \sigma = \sigma^{H} - \left\{1 - \exp\left[-k\left(\dfrac{\varepsilon - \varepsilon_p}{\varepsilon_p}\right)^n\right]\right\}(\sigma_p - \sigma_s) & \varepsilon \geqslant \varepsilon_p \end{cases} \tag{10}$$

Fig. 8 shows a comparison between the measured and predicted flow curves for the present alloy in various deformation conditions. A good agreement is obtained over the entire strain level, indicating that the proposed constitutive model can be implemented to finite element analysis to simulate the hot working of medium entropy alloys. Moreover, the advantages of the present model are evident when compared with the pre-existing models, as follows.

1) As mentioned in Section 1, though the modified hyperbolic-sine law has been widely applied, it is empirical and is only valid within the experimental strain range from which the constitutive expression has been derived. However, the present model is semi-physical-based and can extrapolate the flow curves to strain levels outside the experimental strain range.

2) In comparison with other physical based models[16], there are much fewer material constants in the present model and the regression analysis is much more simplified. One may further speculate that this model not only can be applied for the current medium entropy alloy, but also can be promoted to other metallic materials with low stacking-fault energy.

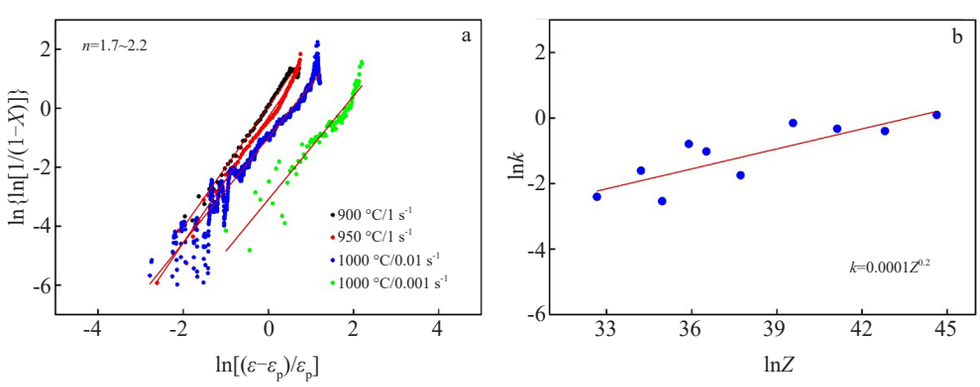

Fig.7 Determination of the parameters k and n in Eq.(9) under various conditions (a) and correlation between k and Z parameter (b)

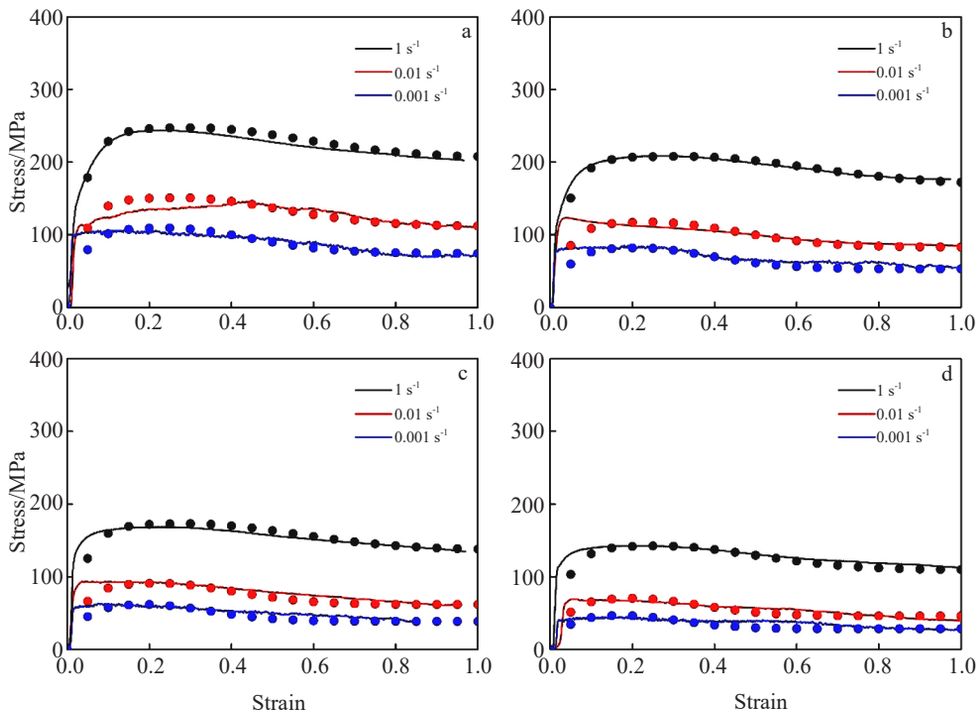

Fig.8 Comparison between the experimental flow curves and the predicted data under various deformation conditions

3 Conclusions

1) Due to the predominance of dynamic recrystallization during deformation, the flow curve exhibits single peak type, which can be divided into two stages, namely the work-hardening stage and the dynamic softening stage. The flow stress is quite sensitive to the deformation temperature and strain rate. With increasing the temperature and decreasing strain rate, the flow stress is evidently decreased.

2) The features of the work-hardening stage can be well-described by the Kocks-Mecking plots. It is found that the hardening rate is linearly decreased with stress, so that the stress-strain behavior can be precisely described based on the conventional dislocation density model.

3) In the dynamic softening regime where the dynamic recrystallization is predominant, the softening kinetics can be modelled by the well-known JMAK equation. The recrystallization kinetics model can accurately predict the flow stress after the peak stress.

References

1 Yeh J W, Chen S K, Lin S J *et al. Adv Eng Mater*[J], 2004(6): 299
2 Zhang Y, Zuo T T, Tang Z *et al. Prog Mater Sci*[J], 2014, 61: 1
3 Varalakshmi S, Kamaraj M, Murty B S. *Materials Science and Engineering A*[J], 2010, 527: 1027
4 Soto A O, Salgado A S, Niño E B. *Intermetallics*[J], 2020, 124: 106 850
5 Pei Zongrui. *Materials Science and Engineering A*[J], 2018, 737: 132
6 He J Y, Wang H, Wu Y *et al. Intermetallics*[J], 2016, 79: 41
7 Lu A Y, Dong Y, Jiang H *et al. Scripta Materialia*[J], 2020, 187: 202
8 Wu Q F, Wang Z J, Zheng T. *Materials Letters*[J], 2019, 253: 268
9 Joseph J, Jarvis T, Wu X H. *Materials Science and Engineering A*[J], 2015, 633: 184
10 Jeong H T, Park H K, Park K *et al. Materials Science and Engineering A*[J], 2019, 756: 528
11 Nayan N, Singh G, Murty S V S N *et al. Intermetallics*[J], 2014, 55: 145
12 Rahul M R, Samal S, Venugopal S *et al. Journal of Alloys and Compounds*[J], 2018, 749: 1115
13 Zhang Y, Li J S, Wang J. *Journal of Alloys and Compounds*[J], 2018, 757: 39
14 Wang Y T, Li J B, Xin Y C *et al. Acta Metallurgica Sinica*[J], 2019, 32: 932
15 Werner R, Lindemann J, Clemens H *et al. BHM*[J], 2014, 159: 286
16 Lin Y C, Chen X M. *Materials and Design*[J], 2011, 32: 1733
17 Liu H Y, Gu C, Zhai K *et al. Vacuum*[J], 2021, 184: 109 995
18 Laasraoui, Jonas J J. *Metallurgical Transactions A*[J], 1991, 22: 1545
19 Bambach M, Sizova I, Bolz S *et al. Metals*[J], 2016, 6: 204

考虑加工硬化和动态软化的FeCrNiMn中熵合金本构模型

梅金娜[1]，薛　飞[1]，吴天栋[2]，卫　娜[2]，蔡　振[1]，薛祥义[2]
(1. 苏州热工研究院有限公司，江苏 苏州 215004)
(2. 西安超晶科技有限公司，陕西 西安 710200)

摘　要：采用等温压缩分析了$Fe_{0.25}Cr_{0.25}Ni_{0.25}Mn_{0.25}$中熵合金在900~1050 ℃、0.001~1 s^{-1}应变速率范围内的流变行为。结果表明，热变形以动态再结晶为主，与其他低堆垛层错能的合金一样，流变曲线呈单峰形状。建立了本构模型来描述整个变形过程，分析了加工硬化行为和动态软化过程。利用Kocks-Mecking图发现，在加工硬化阶段，合金的硬化速率随应力呈线性降低，因此应力-应变行为可以用传统的位错密度模型来描述。同时，采用经典的JMAK方程描述由动态再结晶引起的软化过程。此外，对本构模型进行了进一步的修改，减少了参数的数量，简化了回归分析。所提出的半物理模型不仅可以准确地预测应变范围外的应力-应变行为，而且可用于其他低层错能合金。

关键词：中熵合金；热变形；流变行为；本构模型

作者简介：梅金娜，女，1981年生，高级工程师，苏州热工研究院有限公司，江苏 苏州 215004，电话：029-86066135，E-mail：meijinna@cgnfc.com.cn